The Role of Air–Sea Coupling in Seasonal Prediction of Asia–Pacific Summer Monsoon Rainfall

JIESHUN ZHU

Center for Ocean–Land–Atmosphere Studies, Institute of Global Environment and Society, Calverton, Maryland

JAGADISH SHUKLA

Center for Ocean–Land–Atmosphere Studies, Institute of Global Environment and Society, Calverton, Maryland, and Department of Atmospheric, Oceanic, and Earth Sciences, College of Science, George Mason University, Fairfax, Virginia

(Manuscript received 24 March 2013, in final form 21 May 2013)

ABSTRACT

This study examines the role of the air–sea coupled process in the seasonal predictability of Asia–Pacific summer monsoon rainfall by comparing seasonal predictions from two carefully designed model experiments: tier 1 (fully coupled model) and tier 2 (AGCM with prescribed SSTs). In these experiments, an identical AGCM is used in both tier 1 and tier 2 predictions; the daily mean SSTs from tier 1 coupled predictions are prescribed as a boundary condition in tier 2 predictions. Both predictions start in April from 1982 to 2009, with four ensemble members for each case. The model used is the Climate Forecast System, version 2 (CFSv2), the current operational climate prediction model for seasonal-to-interannual prediction at the National Centers for Environmental Prediction (NCEP). Comparisons indicate that tier 2 predictions produce not only higher rainfall biases but also unrealistically high rainfall variations in the tropical western North Pacific (TWNP) and some coastal regions as well. While the prediction skill in terms of anomaly correlations does not present a significant difference between the two types of predictions, the root-mean-square errors (RMSEs) are clearly larger over the above-mentioned regions in the tier 2 prediction. The reduced RMSE skills in the tier 2 predictions are due to the lack of a coupling process in AGCM-alone simulations, which, particularly, results in an unrealistic SST–rainfall relationship over the TWNP region. It is suggested that for a prediction of summer monsoon rainfall over the Asia–Pacific region, it is necessary to use a coupled atmosphere–ocean (tier 1) prediction system.

1. Introduction

The Asia–Pacific summer monsoon affects more than 60% of the world's population. Monsoon rainfall is a critical factor for food production and human welfare (Parthasarathy et al. 1988). An accurate and reliable monsoon rainfall could be of immense value for local water management and agricultural planning. In a previous study, Charney and Shukla (1981) provided a scientific basis for monsoon prediction beyond the 2-week limit of deterministic predictability that showed that the lower-boundary conditions (e.g., SST) could influence seasonal mean monsoon circulation and rainfall. This concept also provided scientific basis for the predictability of seasonal mean climate anomalies globally. Based on this idea, a substantial amount of research has been conducted to examine the predictability of seasonal mean atmospheric anomalies [see review papers by Palmer and Anderson (1994) and Kang and Shukla (2005)]. It has been particularly successful in identifying the global teleconnections induced by the El Niño–Southern Oscillation (ENSO) cycle (Ropelewski and Halpert 1987; Shukla 1998; Straus et al. 2003).

In real-time forecasts, the boundary conditions, such as SST, should be predicted. Over the years, dynamical seasonal predictions have been conducted by adopting the so-called tier 2 approach (Bengtsson et al. 1993). In this approach, the future state of global SSTs was first predicted either by some simplified dynamical models, coupled ocean–atmosphere general circulation models (CGCMs) with relatively low resolutions, or statistical methods. The predicted SSTs (or SST anomalies) are

Corresponding author address: Jieshun Zhu, COLA, IGES, 4041 Powder Mill Road, Suite 302, Calverton, MD 20705-3106.
E-mail: jieshun@cola.iges.org

DOI: 10.1175/JCLI-D-13-00190.1

then specified as the boundary condition for AGCM integrations. The main advantages of such a "tier 2" system, compared with a high-resolution CGCM, are avoiding the large systematic errors of fully coupled high-resolution models and computational efficiency. With the development of improved coupled models and the availability of modern supercomputer resources, tier 1 prediction systems are being used in several operational centers (Palmer et al. 2004; Saha et al. 2006). However, the tier 2 system is still being used for operational forecasting at several centers (Barnston et al. 2010), and as a tool for climate downscaling.

A major assumption of the tier 2 system is that, given the large heat capacity of the ocean, its response to the atmospheric forcing is much smaller and slower. In the uncoupled AGCM runs, the ocean heat capacity is assumed to be infinitely large and the prescribed SST does not respond to the AGCM change at all. This assumption is quite valid in areas where SST fluctuations are largely determined by the oceanic dynamics, such as the eastern tropical Pacific Ocean. However, it may be problematic in areas where the local air–sea feedback has a strong effect on SST, such as the "warm seas" in the western Pacific and Indian Oceans. In these regions, SST fluctuations are affected by the atmospheric fluctuations, which in turn modify the atmospheric systems (Wang et al. 2005; Wu and Kirtman 2005). This kind of feedback can be important to produce relatively long-living and potentially predictable signals in the ocean–atmosphere system. In such situations, it is conceivable that a prescribed SST anomaly, without responding to any feedback, is likely to exaggerate its influence on the atmosphere. In fact, studies have demonstrated the vital role of air–sea interaction in the monsoon regions (Fu et al. 2002; Wu and Kirtman 2004, 2005, 2007; Wu et al. 2006; Wang et al. 2005; Cherchi and Navarra 2007; Chen et al. 2012; Hendon et al. 2012; Hu et al. 2012). For example, Wu and Kirtman (2004) showed the critical role of Indian Ocean coupling in maintaining the relationship between the Indian summer monsoon and ENSO. Wang et al. (2005) identified fundamental discrepancies between SST-forced AGCM simulations and observations. In AGCMs, positive SST–rainfall correlations are found during the summer season, especially over the western Pacific region, which is opposite of the observations. They have argued that a coupled ocean–atmosphere model is required for the simulation and prediction of precipitation over the Asia–Pacific monsoon region. Generally, these studies pointed out the deficiencies of the tier 2 system about the lack of coupling feedback.

However, few studies have compared the tier 1 and tier 2 systems in a prediction mode. Kug et al. (2008) conducted a comparison study in which two different AGCMs (at least in their resolutions) and different anomalous SSTs were used, which makes the comparison problematic. Kumar et al. (2008) made a similar comparison by using the same AGCM and SST anomalies but with different SST climatology, and found that much of the difference was related to the different SST climatology. In fact, most of sensitivity experiments mentioned in the above paragraph also failed in using the same SSTs, and thus the derived conclusions might not be as robust as expected. Therefore, a strict comparison between the tier 1 and tier 2 systems will not only have practical values, but also scientific benefits. In this study, we carry out a strict comparison by a state-of-the-art coupled forecast model, the Climate Forecast System, version 2 (CFSv2)—the current operational climate prediction model for seasonal-to-interannual prediction at the National Centers for Environmental Prediction (NCEP). To make our comparison between the tier 1 and tier 2 predictions more robust, an identical AGCM is used in both tier 1 and tier 2 predictions, and the daily mean SSTs from the tier 1 prediction are used as a boundary condition in the tier 2 prediction. We will focus on the seasonal prediction of Asia–Pacific summer monsoon rainfall.

2. Model, datasets, and prediction experiments

The coupled forecast model used in this study is CFSv2 (Saha et al. 2013, manuscript submitted to *J. Climate*). In CFSv2, the ocean model is the Geophysical Fluid Dynamics Laboratory (GFDL) Modular Ocean Model (MOM), version 4, which is configured for the global ocean with a horizontal grid of $0.5° \times 0.5°$ poleward of 30°S and 30°N and a meridional resolution increasing gradually to 0.25° between 10°S and 10°N. The vertical coordinate is geopotential (z-) with 40 levels (27 of them in the upper 400 m). The maximum depth is approximately 4.5 km. The atmospheric model is a lower-resolution version of the Global Forecast System (GFS), which has a horizontal resolution at T126 (105-km grid spacing) and 64 vertical levels in a hybrid sigma-pressure coordinate. The oceanic and atmospheric components exchange surface momentum, heat and freshwater fluxes, as well as SST, every 30 min.

The tier 1 seasonal prediction is carried out using the coupled model—CFSv2. The ocean initial conditions (OICs) are based on the ocean states from the European Centre for Medium-Range Weather Forecasts (ECMWF) Ocean Reanalysis System 4 (ORA-S4; Balmaseda et al. 2013). For each OIC, four ensemble members are generated by changing their atmospheric and land initial conditions, which are the instantaneous fields from 0000 UTC of the first 4 days in April of each year in the NCEP Climate Forecast System Reanalysis (CFSR; Saha et al. 2010).

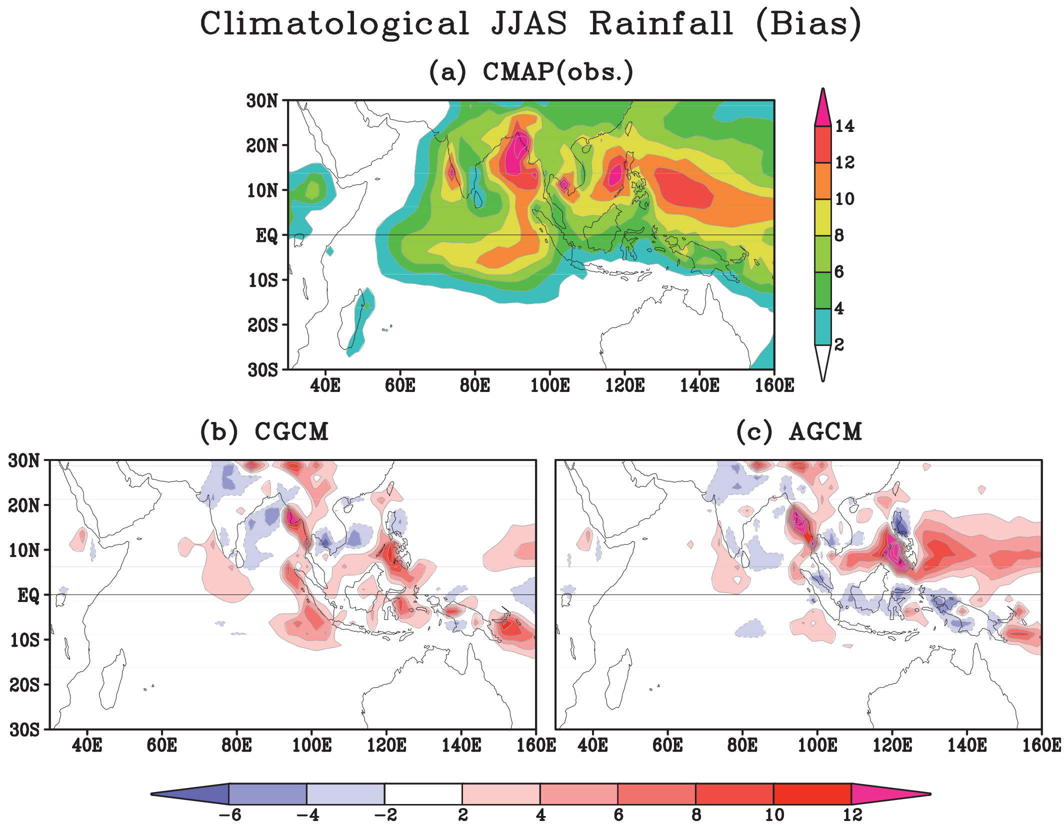

FIG. 1. Climatological JJAS rainfall in (a) CMAP observations, and the climatological biases relative to (a) in (b) CGCM prediction and (c) AGCM prediction. Contour interval is 2 mm day^{-1}.

The experimental predictions are conducted for six months—from April to September—for the period 1982–2009. This experiment is referred to as CGCM prediction. In a previous study, we compared the impact of CFSR and ECMWF ORA-S4 ocean initial conditions, and found that using ECMWF ORA-S4 ocean initial conditions in CFSv2 produces better predictions of SST, especially in the eastern Pacific (Zhu et al. 2012).

For the tier 2 seasonal prediction (referred to as AGCM prediction), daily SST boundary conditions are prescribed from the CGCM prediction. A similar strategy was also used by Kim et al. (2010) to explore the role of air–sea coupling on Madden–Julian oscillation (MJO) predictions, where AGCM was forced with daily SSTs interpolated from pentad mean CGCM SSTs. In the AGCM prediction, there are four ensemble members as well; for each member (say, the second April cases), the same atmospheric and land initial conditions as in CGCM are used to initialize the atmospheric component of CFSv2, which is forced by the daily mean SST from the corresponding CGCM prediction (i.e., the second April cases). Thus, on the daily time scale, the SST is identical between the tier 1 and tier 2 predictions. In the CGCM there is a higher-frequency coupling process, where air–sea fluxes exchange every 30 min. For both predictions, four ensemble members are averaged before comparison.

Monthly rainfall from the National Oceanic and Atmospheric Administration's (NOAA) Climate Prediction Center Merged Analysis of Precipitation (CMAP) (Xie and Arkin 1997) is used as a proxy for rainfall observations, which is on a 2.5° × 2.5° grid.

3. Results

Figure 1 shows the 28-yr mean (1982–2009) climatological monsoon [June–September (JJAS)] rainfall from observations (Fig. 1a) and model biases relative to the observations in the two types of predictions (Figs. 1b,c). The observed mean seasonal precipitation (Fig. 1a) is generally above 6 mm day^{-1} to the east of 60°E and north of 10°S over the tropical Indian Ocean, and covers a large area of the western Pacific and the Asian continent. Climatological precipitation in this area is characterized by an array of heavy rainfall centers lined up in the northern latitudinal zone between 10° and 20°N, near the western coast of India; the northeastern part of the Bay of Bengal;

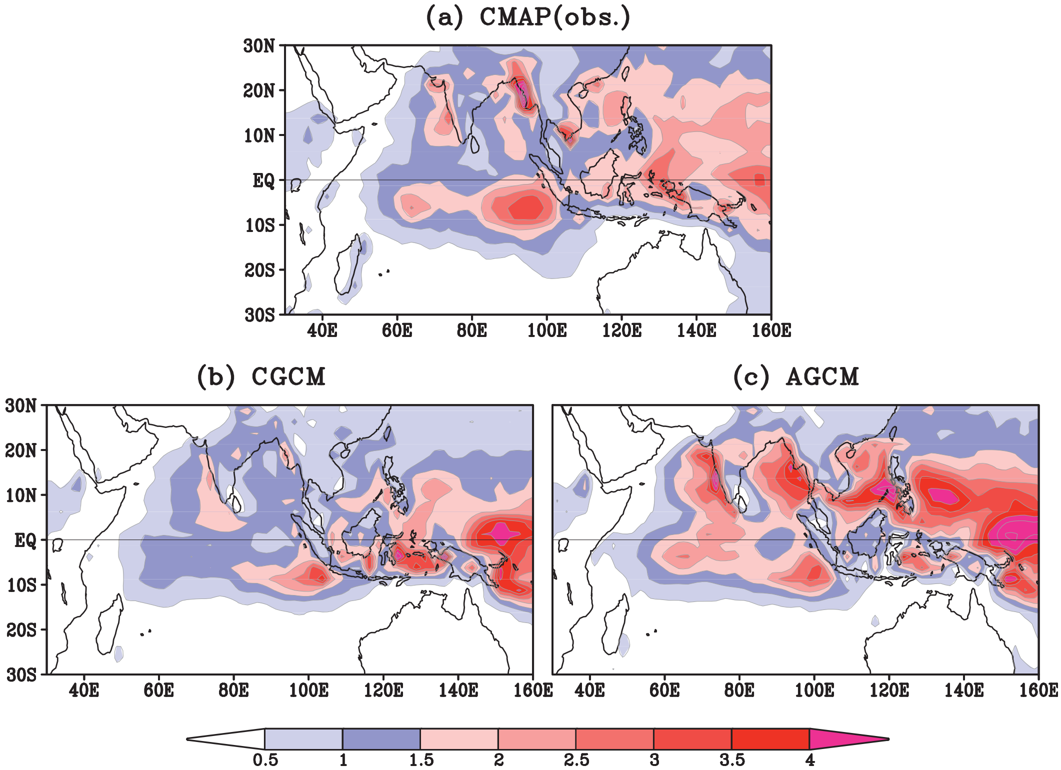

FIG. 2. Standard deviation of JJAS rainfall anomalies in (a) CMAP observations, (b) CGCM prediction, and (c) AGCM prediction. Contour interval is 0.5 mm day^{-1}.

and both the eastern and western sides of the Philippines, in the eastern South China Sea and western Pacific. Another southern belt of heavy precipitation is between 10°S and the equator, extending from the Sumatra coast and further westward in the Indian Ocean.

Although the major features of the observed mean precipitation are captured by both predictions qualitatively (not shown), there are substantial model biases (Figs. 1b,c). In the CGCM prediction (Fig. 1b), systematic biases are dominated by relatively large errors in the coastal regions, such as the wet biases to the west of the Philippines and west of the Indochina Peninsula and dry biases over west of the Bay of Bengal and northern India. For the AGCM prediction (Fig. 1c), the bias pattern is also similar over the Indian Ocean and South Asia, with the wet biases near the eastern Bay of Bengal somewhat enlarged, while the dry biases are generally weakened. The most striking difference, however, appears in the tropical western North Pacific (TWNP; 5°–20°N, 110°–160°E), where not only the wet bias to the west of Philippines is enhanced, in comparison to its coupled counterparts (Figs. 1b), but much larger wet biases are found over the ocean to the east of the Philippines in the western Pacific. This is in contrast to the results reported by Kug et al. (2008), who did not find significant differences in precipitation between the coupled and uncoupled simulations. In their case, however, different AGCMs and different SSTs were used in the tier 1 and tier 2 experiments, making the comparison problematic.

The differences between the coupled and uncoupled predictions are more clearly demonstrated by the magnitudes and the patterns of interannual standard deviations of seasonal rainfall anomalies (Fig. 2). The observations (Fig. 2a) show that large interannual anomalies generally overlap with the major centers of the mean precipitation, except for the equatorial western Pacific, where ENSO causes large interannual rainfall variations. The general features of observed interannual variability are well captured by the CGCM (Fig. 2b), except for generally lower standard deviations for the centers in the Indian Ocean basin, the eastern Bay of Bengal, and the northwestern Pacific. In contrast, the AGCM predictions (Fig. 2c) show large discrepancies. The amplitude of variability is significantly larger than that from both the observations and the couple model. It is more than twice in the centers of the active regions. If the standard deviations were calculated for each prediction member individually and then averaged, the differences would be even larger (not shown). This difference implies that coupling plays an important ''damping'' role in these regions, which suppresses the

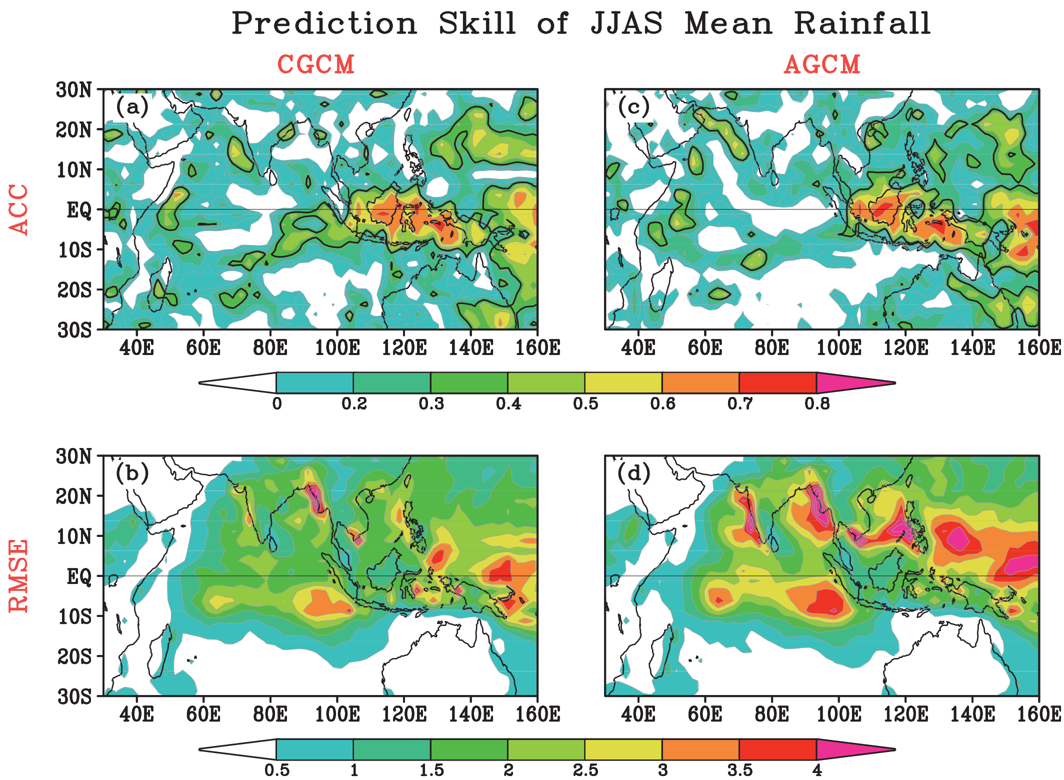

FIG. 3. Prediction skill of JJAS rainfall for (a),(b) CGCM prediction and (c),(d) AGCM prediction for (top) anomaly correlation coefficients and (bottom) RMSE. Contour interval is (a),(c) 0.1 and (b),(d) 0.5 mm day^{-1}. In (a) and (c), ACCs larger than 0.32 (black contour) are significant at the 95% confidence level, according to the one-tailed Student's t test (DOF = 26).

atmospheric response to SST. This is particularly true in the TWNP region.

The patterns of the JJAS precipitation prediction skill are shown in Fig. 3 in terms of anomaly correlation coefficients (ACCs; top panels) and root-mean-square errors (RMSEs; bottom panels). The ACC maps (Figs. 3a,c) show that most of the model skill is concentrated in the equatorial regions in the western Pacific and the Maritime Continent, which should be related to SST variations in the eastern tropical Pacific and thus there is no clear difference between the ACC patterns for the CGCM and AGCM predictions. Other regions of relatively higher skills include the northwestern Pacific and near the western coast of India, both between 10° and 20°N. The CGCM prediction also shows somewhat higher skill in the eastern equatorial Indian Ocean than the AGCM prediction. In general, however, the ACC difference is insignificant between the two predictions in these areas.

The RMSE maps (Figs. 3b,d) show large errors for the AGCM compared to the CGCM predictions. The RMSE patterns from the two predictions are similar to their respective interannual variation patterns (e.g., Figs. 2b,c). The AGCM prediction errors (Fig. 3d) are above 3 mm day^{-1} over a large region stretching from the west coast of India to the western Pacific. These errors are substantially larger than those in the CGCM prediction (Fig. 3c). For instance, the difference between the CGCM and AGCM predictions were much larger for the 1997 El Niño year (Fig. 4), for which severe droughts were predicted over India by the AGCM prediction, but they were not seen in observations and were weaker in the CGCM predictions.

Figure 5 shows pattern correlations and RMSEs for JJAS precipitation over the domain (30°S–30°N, 30°–160°E) during 1982–2009. Correlations are comparable in both predictions, with the mean correlation being 0.22 and 0.19 for the CGCM and AGCM predictions, respectively. In contrast, RMSEs are generally always higher for the AGCM compared to the CGCM.

4. Discussion

During the past 30 years, a large number of AGCM experiments have been carried out with prescribed SST (Gates et al. 1999; and many others). These numerical experiments were helpful in establishing the role of

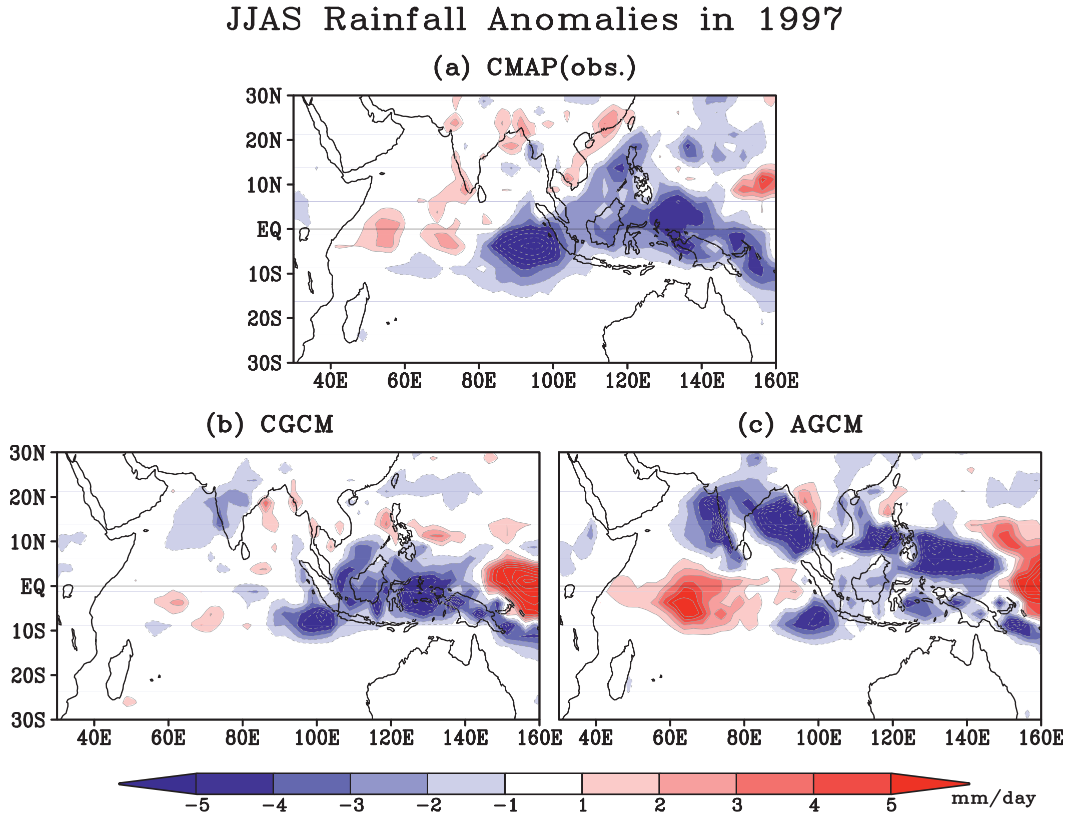

FIG. 4. Distribution of JJAS rainfall anomalies in 1997 from (a) observations (CMAP), (b) CGCM prediction, and (c) AGCM prediction. Contour interval is 1 mm day^{-1}.

slowly varying boundary conditions of SST in forcing the atmospheric circulations and rainfall. AGCMs were so successful in simulating the observed atmospheric tropical circulation in response to observed large SST anomalies in the tropical Pacific associated with ENSO, which helped establish a scientific basis for dynamical seasonal predictions (Shukla 1998; Kang and Shukla 2005). Nevertheless, it was noted (Wu and Kirtman 2004; Wang et al. 2005) that the regional atmospheric circulation and rainfall over the Indian Ocean and especially over the western Pacific region, in response to the prescribed observed SST, were quite unrealistic in the summer season. The present study was designed to address this issue systematically. Both coupled model forecasts and, AGCM forecasts are compared with observations, and AGCM forecasts forced by SSTs from the coupled model forecasts.

Wang et al. (2005) had shown (and confirmed by our study as in Fig. 6) that the correlation between SST and rainfall over the tropical western North Pacific region was negative in observations and coupled models, but positive in AGCM simulations. In AGCM simulations, where SST is unable to respond to atmospheric fluctuations, there is no control (damping) on fluxes at the ocean–atmosphere interface. If the convection parameterization in the model is such that it produces convective rainfall in response to warmer SST anomalies, then the model will produce a positive correlation between SST and rainfall. However, in reality, warm SST may not produce convection because of two reasons: 1) the region of warm SST may be under the influence of large-scale descending motion caused by convection elsewhere and 2) the local warm (cold) SST anomaly might have been produced by absence (presence) of cloudiness and weak (strong) winds (in other words, the local warm SST is a result of atmospheric forcing). For the Indian Ocean and the western Pacific region, both processes seem to be important. TWNP is clearly an example of a region where SST changes are mainly driven by cloudiness and wind anomalies in the overlying atmosphere. The cloudiness affects the shortwave radiation reaching the ocean surface, and wind anomalies affect evaporation from the ocean. Both processes are also noticed by Wu and Kirtman (2005).

The lack of damping of fluxes in our uncoupled AGCM integrations is clearly seen in unrealistically

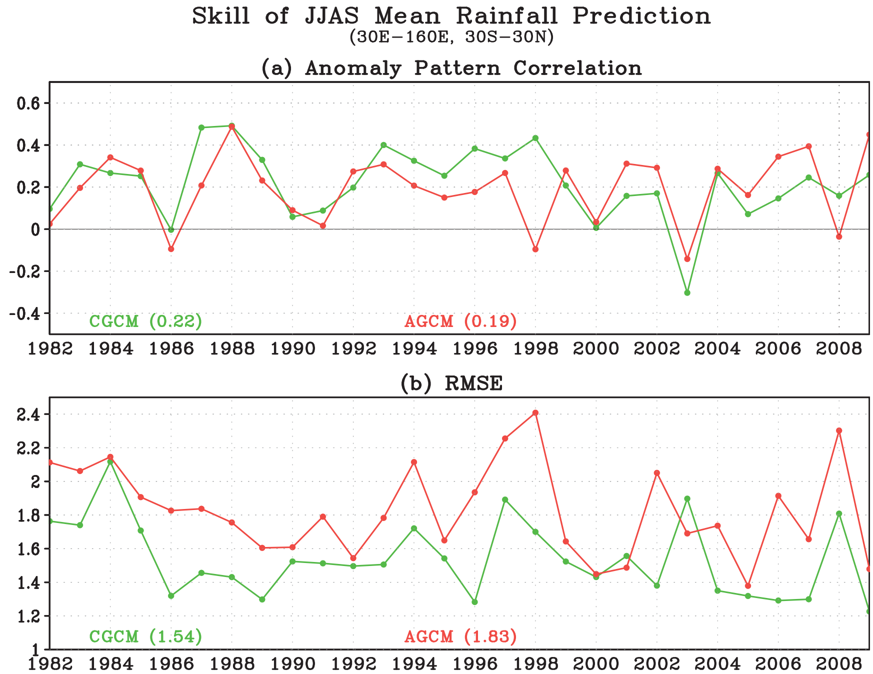

FIG. 5. (a) Anomaly pattern correlation and (b) pattern RMSE (mm day^{-1}) of JJAS rainfall from CGCM prediction (green) and AGCM prediction (red) over the domain (30°S–30°N, 30°–160°E) during 1982–2009. Numbers in brackets are the mean values averaged over 1982–2009.

large values of standard deviation of precipitation (Fig. 2). This is even more evident when we investigate the time series of regional mean precipitation (not shown), where both floods and droughts were far more severe in the AGCM integration compared to the coupled integrations. These results suggest that a hybrid approach, where SST is prescribed over those regions where the atmosphere is strongly forced by the underlying SST and a coupled or mixed-layer model with high (~1 m) vertical resolution in the upper ocean is used in those regions where SST is forced by the overlying atmosphere, may provide better skill in seasonal prediction of summer monsoon rainfall. The high vertical resolution will be able to resolve the diurnal cycle, which plays an important role in this region (Woolnough et al. 2007). The hybrid approach will also benefit some less developed countries that cannot afford a fully coupled model for seasonal prediction.

5. Conclusions

In this study, two sets of carefully designed prediction experiments are conducted to examine the role of air–sea coupling in the seasonal predictability of Asia–Pacific summer monsoon rainfall. The predictions are conducted by both tier 1 and tier 2 forecast systems based on CFSv2, starting from each April during 1982–2009, with four ensemble members for each case. The experiments are designed to ensure that 1) exactly the same AGCM is used in both tier 1 and tier 2 predictions, and 2) exactly the same daily mean SSTs are used in the tier 2 prediction that were generated by the tier 1 system. Comparing the tier 1 and tier 2 predictions, the following differences are found:

- In the absence of air–sea coupling, tier 2 predictions produce higher rainfall biases and unrealistically high rainfall interannual variations.
- The prediction skill, as measured by anomaly correlation, does not show significant differences between the two types of predictions, but RMSEs are significantly larger for the AGCM (tier 2) predictions compared to the CGCM (tier 1) predictions.

These results suggest that coupled ocean–atmosphere models are the most promising tools for operational prediction of seasonal mean rainfall over the Asia–Pacific region. Development of high-fidelity coupled ocean–atmosphere models and consistent initial conditions of ocean, land, and atmosphere are required to realize the potential predictability of seasonal variations. In addition, this study is based on one system that can represent air–sea coupling processes relatively well (Fig. 6).

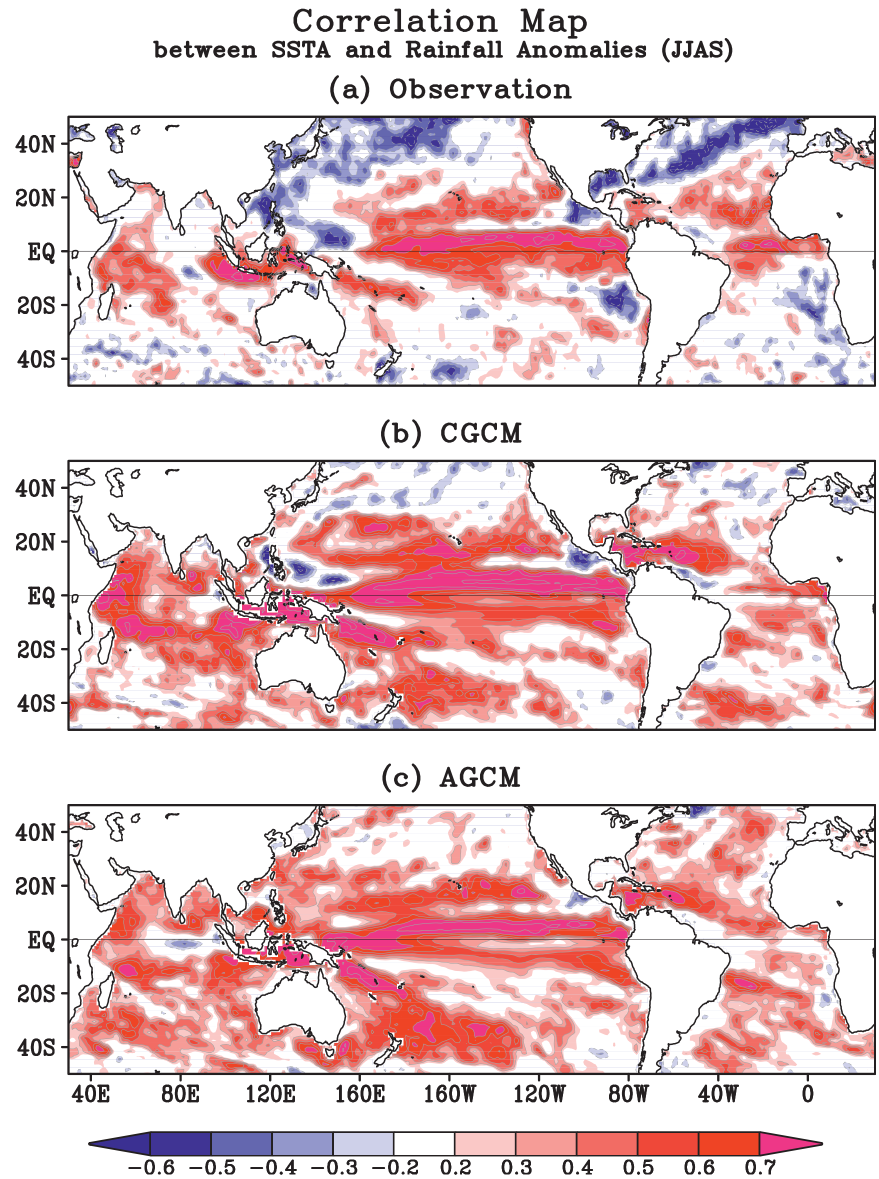

FIG. 6. Correlation coefficients between SST anomalies and rainfall anomalies during the summer monsoon season (JJAS) for (a) observations, (b) CGCM, and (c) AGCM.

We are urging more similar comparisons based on different systems to confirm our findings.

Acknowledgments. Funding for this study was provided by NSF (Grant ATM-0830068), NOAA (Grant NA09OAR4310058), and NASA (Grant NNX09AN50G). Helpful comments from Drs. B. Huang, E. K. Schneider, R. Wu, and Ms. H. Chen are highly appreciated. We thank Dr. B. Huang for carefully reading the early manuscript. We also thank Dr. M. A. Balmaseda from ECMWF for providing its ocean initial conditions and L. Marx for help in the experiment setup. Computing resources provided by the NASA Advanced Supercomputing (NAS) division are also gratefully acknowledged.

REFERENCES

Balmaseda, M. A., K. Mogensen, and A. T. Weaver, 2013: Evaluation of the ECMWF ocean reanalysis system ORAS4. *Quart. J. Roy. Meteor. Soc.,* doi:10.1002/qj.2063, in press.

Barnston, A. G., S. Li, S. J. Mason, D. G. DeWitt, L. Goddard, and X. Gong, 2010: Verification of the first 11 years of IRI's seasonal climate forecasts. *J. Appl. Meteor. Climatol.,* **49,** 493–520.

Bengtsson, L., U. Schlese, E. Roeckner, M. Latif, T. Barnett, and N. Graham, 1993: A two-tiered approach to long-range climate forecasting. *Science,* **261,** 1026–1029.

Charney, J. G., and J. Shukla, 1981: Predictability of monsoons. *Monsoon Dynamics,* J. Lighthill and R. P. Pearce, Eds., Cambridge University Press, 99–109.

Chen, M., W. Wang, A. Kumar, H. Wang, and B. Jha, 2012: Ocean surface impacts on the seasonal-mean precipitation over the tropical Indian Ocean. *J. Climate,* **25,** 3566–3582.

Cherchi, A., and A. Navarra, 2007: Sensitivity of the Asian summer monsoon to the horizontal resolution: Differences between AMIP-type and coupled model experiments. *Climate Dyn.,* **28,** 273–290.

Fu, X., B. Wang, and T. Li, 2002: Impacts of air–sea coupling on the simulation of the mean Asian summer monsoon in the ECHAM4 model. *Mon. Wea. Rev.,* **130,** 2889–2904.

Gates, W. L., and Coauthors, 1999: An overview of the results of the Atmospheric Model Intercomparison Project (AMIP I). *Bull. Amer. Meteor. Soc.,* **80,** 29–56.

Hendon, H. H., E.-P. Lim, and G. Liu, 2012: The role of air–sea interaction for prediction of Australian summer monsoon rainfall. *J. Climate,* **25,** 1278–1290.

Hu, Y., Z. Zhong, X. Liu, and Y. Zhu, 2012: Influence of air–sea interaction on the simulation of the East Asian summer monsoon: A case study. *Dyn. Atmos. Oceans,* **53–54,** 1–16.

Kang, I.-S., and J. Shukla, 2005: Dynamic seasonal prediction and predictability of the monsoon. *The Asian Monsoon,* B. Wang, Ed., Springer Praxis, 585–612.

Kim, H. M., C. D. Hoyos, P. J. Webster, and I. S. Kang, 2010: Ocean-atmosphere coupling and the boreal winter MJO. *Climate Dyn.,* **35,** 771–784.

Kug, J.-S., I.-S. Kang, and D.-H. Choi, 2008: Seasonal climate predictability with tier-one and tier-two prediction systems. *Climate Dyn.,* **31,** 403–416.

Kumar, A., Q. Zhang, J.-K. E. Schemm, M. L'Heureux, and K.-H. Seo, 2008: An assessment of errors in the simulation of atmospheric interannual variability in uncoupled AGCM simulations. *J. Climate,* **21,** 2204–2217.

Palmer, T. N., and D. L. T. Anderson, 1994: The prospects for seasonal forecasting—A review paper. *Quart. J. Roy. Meteor. Soc.,* **120,** 755–793.

——, and Coauthors, 2004: Development of a European Multimodel Ensemble System for Seasonal-to-Interannual Prediction (DEMETER). *Bull. Amer. Meteor. Soc.,* **85,** 853–872.

Parthasarathy, B., A. A. Munot, and D. R. Kothawale, 1988: Regression model for estimation of Indian food grain production from Indian summer rainfall. *Agric. For. Meteor.,* **42,** 167–182.

Ropelewski, C. F., and M. S. Halpert, 1987: Global and regional scale precipitation patterns associated with the El Niño/Southern Oscillation. *Mon. Wea. Rev.,* **115,** 1606–1626.

Saha, S., and Coauthors, 2006: The NCEP Climate Forecast System. *J. Climate,* **19,** 3483–3517.

——, and Coauthors, 2010: The NCEP Climate Forecast System Reanalysis. *Bull. Amer. Meteor. Soc.,* **91,** 1015–1057.

Shukla, J., 1998: Predictability in the midst of chaos: A scientific basis for climate forecasting. *Science,* **282,** 728–731.

Straus, D., J. Shukla, D. Paolino, S. Schubert, M. Suarez, P. Pegion, and A. Kumar, 2003: Predictability of the seasonal mean atmospheric circulation during autumn, winter, and spring. *J. Climate,* **16,** 3629–3649.

Wang, B., Q. Ding, X. Fu, I.-S. Kang, K. Jin, J. Shukla, and F. Doblas-Reyes, 2005: Fundamental challenge in simulation and prediction of summer monsoon rainfall. *Geophys. Res. Lett.,* **32,** L15711, doi:10.1029/2005GL022734.

Woolnough, S. J., F. Vitart, and M. A. Balmaseda, 2007: The role of the ocean in the Madden–Julian oscillation: Implications for MJO prediction. *Quart. J. Roy. Meteor. Soc.,* **133,** 117–128.

Wu, R., and B. P. Kirtman, 2004: Impacts of the Indian Ocean on the Indian summer monsoon–ENSO relationship. *J. Climate,* **17,** 3037–3054.

——, and ——, 2005: Roles of Indian and Pacific Ocean air–sea coupling in tropical atmospheric variability. *Climate Dyn.,* **25,** 155–170.

——, and ——, 2007: Regimes of seasonal air–sea interaction and implications for performance of forced simulations. *Climate Dyn.,* **29,** 393–410.

——, ——, and K. Pegion, 2006: Local air–sea relationship in observations and model simulations. *J. Climate,* **19,** 4914–4932.

Xie, P., and P. A. Arkin, 1997: Global precipitation: A 17-year monthly analysis based on gauge observations, satellite estimates, and numerical model outputs. *Bull. Amer. Meteor. Soc.,* **78,** 2539–2558.

Zhu, J., B. Huang, L. Marx, J. L. Kinter III, M. A. Balmaseda, R.-H. Zhang, and Z.-Z. Hu, 2012: Ensemble ENSO hindcasts initialized from multiple ocean analyses. *Geophys. Res. Lett.,* **39,** L09602, doi:10.1029/2012GL051503.